In situ fabrication of alumina nanotube array and photoluminescence

G. S. Huang, X. L. Wu,[a] F. Kong, and Y. C. Cheng
National Laboratory of Solid State Microstructures, Nanjing University, Nanjing 210093, People's Republic of China and Department of Physics, Nanjing University, Nanjing 210093, People's Republic of China

G. G. Siu and Paul K. Chu
Department of Physics and Materials Science, City University of Hong Kong, Kowloon, Hong Kong, People's Republic of China

(Received 5 March 2006; accepted 28 June 2006; published online 17 August 2006)

Aluminum foil was anodized in aged electrolyte under high voltage. The morphology observation shows that the alumina film has a three-layer structure from bottom to top and the middle layer shows large quantities of individual alumina nanotubes. Their formation mechanism is discussed in detail. Under ultraviolet excitation, the alumina film exhibits an emission centered at ~400 nm. Based on annealing behavior of the emission band and electron paramagnetic resonance result, the origin of the emission is considered to be due to optical transition in single ionized oxygen vacancy (F^+ center) in the alumina. The experimental results can be expected to have favorable applications in optoelectronics and biotechnology. © *2006 American Institute of Physics*.
[DOI: 10.1063/1.2337160]

In recent years, there has been a growth of attention in synthesis of well-organized one-dimensional (1D) nanomaterials. Simple and convenient fabrication of 1D nanomaterials using porous anodic alumina (PAA) membrane as a template has thus attracted more and more interest.[1–5] Corresponding alumina nanotube (ANT), as a special nanostructure with high flexibility[6] and important dielectric properties,[7] can be considered as outer insulating protective layer and has been proposed to synthesize with several methods, such as anodization of Si-based Al film,[8] chemical etching in NaOH solution,[9] and ultrasonic treatment of PAA membrane.[10] However, these methods have obvious disadvantages such as short lengths of obtained nanotubes, fussy processes, inevitable introduction of impurity, and low productivity. These shortcomings have limited more applications of the ANTs. Recently, Chu *et al.*[11] have reported fabrication of the PAA membrane with ordered nanopore array under high voltage in an aged electrolyte, which leads to the birth of an expanded field of PAA-related materials. In this letter, we report *in situ* fabrication of large quantities of ANTs without any additional post-treatment. The convenient fabrication method provides a good basis for seeking further applications of the ANTs. In addition, we found that the obtained ANT array has an obvious blue photoluminescence (PL) under ultraviolet excitation. The PL mechanism is discussed in detail on the basis of its annealing behavior.

Anodization of high-purity Al foil (99.99%) was conducted in an aged 15 wt % sulfuric acid solution which underwent a preanodization for 15 A h. This aging treatment of the electrolyte can enhance breakdown potential of PAA membrane prominently.[11] During the anodization, the solution temperature was maintained at 5 °C. The anodization was initially carried out at constant current. And the applied voltage begins from zero to a preset value and then remains unchanged for 1 h. The obtained products are classified as three groups, A, B, and C. They correspond to the preset voltages of 60, 50, and 40 V, respectively, and a subscript such as 190 in A_{190} is used to designate the initial current density (mA/cm^2). The surface morphologies were characterized using field emission scanning electron microscope (SEM, LEO 1530VP). PL and PL excitation (PLE) spectra were taken on Fluoromax-2 fluorescence spectrometer (Jobin-Yvon Company). Electron paramagnetic resonance (EPR) spectra were obtained with a Bruker EMX-10/12 spectrometer. All the measurements were run at room temperature.

Figure 1(a) shows the SEM image of sample A_{190}. A three-layer-structure morphology can clearly be observed.

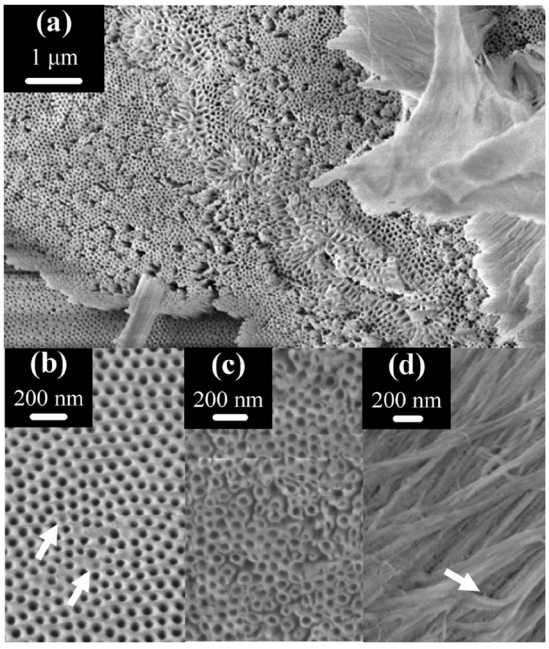

FIG. 1. (a) SEM image of sample A_{190}. A unique three-layer structure can be clearly observed. The corresponding enlarged images of the three layers are displayed in (b), (c), and (d), respectively.

[a]Author to whom correspondence should be addressed; electronic mail: hkxlwu@nju.edu.cn

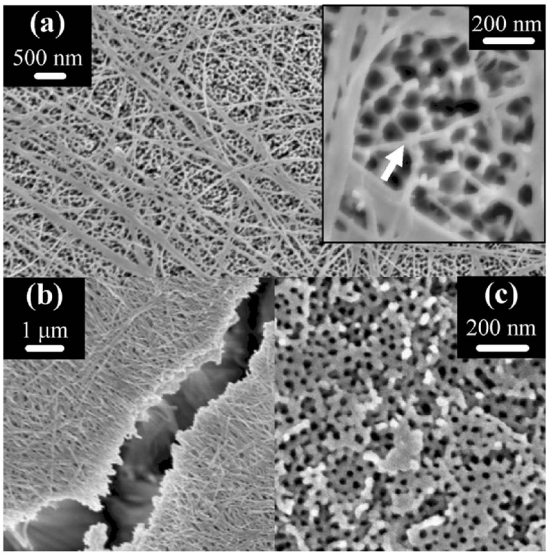

FIG. 2. (a) SEM image of sample C_{175}. The inset shows an enlarged image. (b) SEM image of sample B_{175}. (c) SEM image of sample C_{150}.

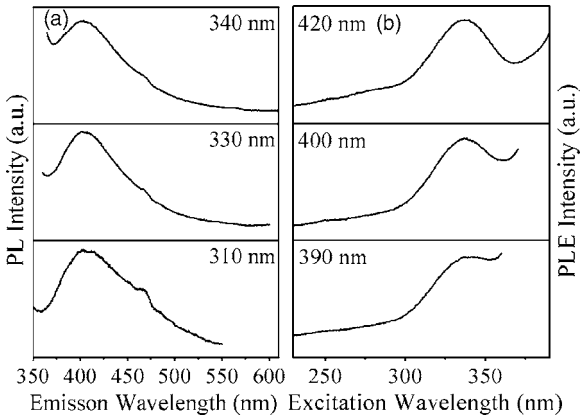

FIG. 3. (a) PL spectra of sample B_{175}, taken under excitation with the 310, 330, and 340 nm lines of a Xe lamp. (b) PLE spectra of sample B_{175}, taken by monitoring at the 390, 400, and 410 nm emission wavelengths.

The bottom layer (lower left corner) is alumina nanopore array. Its enlarged image is shown in Fig. 1(b). The nanopore array shows a density-packed hexagonal structure. In our previous results,[12] some protuberances were observed on the boundaries of some ordered areas and considered to be due to the suspension formed under internal stress.[13] However, the current morphology demonstrates concaves instead of convexes on the boundaries [see the white arrows in Fig. 1(b)]. This feature indicates that the pore growth is rapid and has not totally stopped under high voltage. The middle layer can be seen to be individual ANT arrays [see the enlarged image in Fig. 1(c)]. Large quantities of ANTs with inner and outer diameters of ~65 and ~110 nm, respectively, have *in situ* been formed in this layer. The top layer [the right side in Fig. 1(a)] and its enlarged view in Fig. 1(d) contain bundles of collapsed ANTs. Some curly ANTs illuminate their high flexibility (see the white arrow). These morphology features confirm that this simple method is convenient for bulk production of individual ANTs.

Obviously, the formation of the current ANTs is tightly related to high anodic voltage and large current density used during the anodization. When Al foil was anodized, massive joule heat causes abrupt rise of local temperature of the PAA membrane, which largely accelerates chemical etching of the membrane in such a strong acidic solution (H^+ concentration of the aged electrolyte is about 1*M* with *p*H meter) and thus results in a unique cleavage of the PAA membrane, i.e., the formation of massive ANTs. The alumina nanopores in the bottom layer are less affected by the strong chemical etching and therefore their morphologies almost keep unchanged [Fig. 1(b)]. To further clarify the formation mechanism of the ANTs, the PAA membranes formed under different voltages and current densities were characterized by SEM and the obtained images are displayed in Fig. 2. One can see that the surface-collapsed ANTs can also be observed from sample B_{175} with a thin top layer [Fig. 2(b)], but compared with those from sample A_{190} [Fig. 1(d)], the collapsed ANTs are reduced in quantity and the underneath nanopores/tubes become vaguely visible. For samples C_{175} and C_{150}, the top layer is even thinner [Fig. 2(a)] and almost disappears [Fig. 2(c)]. These results indicate that joule heat produced by chemical etching under high voltage/large current density is a key factor in forming large quantity of ANTs. Here we would like to mention that the temperature of the electrolyte in the experiment by Chu *et al.* was set at a much lower value,[11] which leads to a remarkably reduced chemical etching rate. This results in formation of bare ANTs. In addition, we found that longer anodic time in our present work is also an important factor for fabrication of a lot of ANTs. From Fig. 2(c) and the inset of Fig. 2(a), we can see that some nanopore walls are broken along the channels. This leads to the formation of some slender alumina nanowires (see the white arrow).[10] This result indicates that the ANTs in these samples are different from those in sample A_{190}. According to previous literature,[6,8,10] we know that two different cleavage fashions of PAA membrane can lead to the formation of two kinds of ANTs. One forms the ANTs with smooth outer surface, as observed from sample A_{190}.[8] The other forms the ANTs with resident tube walls by the sacrifice of six neighbor nanopores, which is accompanied with the formation of alumina nanowires.[10] Our present work clearly shows the existence of the two cleavage fashions in the anodizing process of Al foil. So we may control the morphology of the ANTs by adopting appropriate parameters.

PL of the alumina membrane is interesting. We found that although different samples have different morphologies, all the samples show a similar blue PL band under ultraviolet excitation. Figure 3(a) displays the PL result from sample B_{175}. A strong PL band appears at ~400 nm. Its peak position hardly changes with excitation wavelength. The corresponding PLE spectra show a pinned peak at ~335 nm [Fig. 3(b)]. The PL and PLE properties are completely different from those from ordinary PAA membranes formed in sulfuric acid (not shown).[12] Hence, we can rule out the possibility for the PL band to be due to SO_4^{2-} group. To disclose the origin of the PL band, sample B_{175} was annealed at 400 °C in N_2 for 0.5 h. Figure 4(a) and its inset show the PL and PLE spectra of the annealed sample, respectively. It can be seen that the intensities of the ~400 nm PL and ~335 nm PLE bands are dramatically decreased. This suggests that the PL band cannot originate from optical transition in OH^- group, because the intensity of an emission from OH^- group should remarkably be increased in the sample annealed at 400 °C.[14] Figure 4(b) shows the PL spectra of the samples formed under different voltages. We can see that although the two spectra have identical PL peak positions, the PL intensity

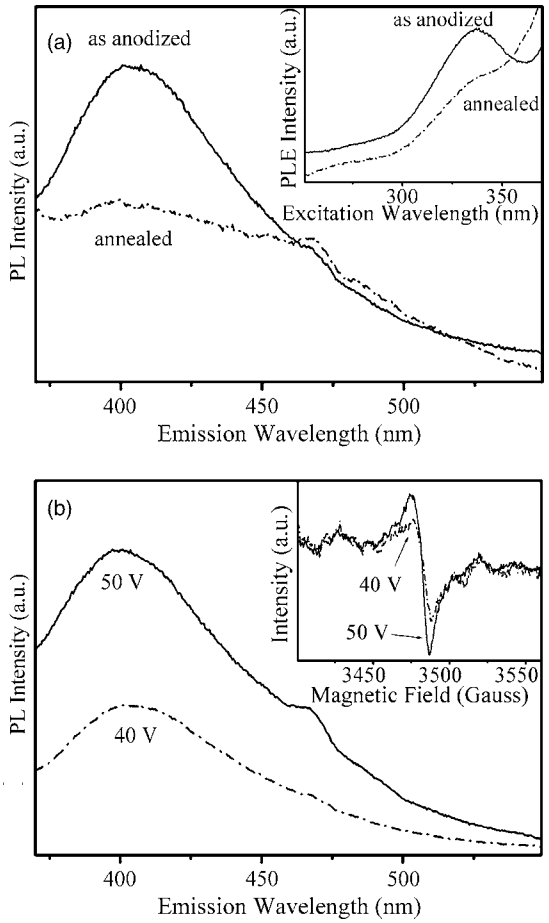

FIG. 4. (a) Annealing behavior of the blue PL band, taken under excitation with the 330 nm line of a Xe lamp. The inset shows annealing behavior of the PLE band, taken by monitoring at 400 nm. (b) PL spectra of samples B_{175} and C_{175}. The inset shows the corresponding EPR spectra.

is stronger in the sample formed under higher anodic voltage. This implies that the sample formed under high voltage has high concentration of luminescent centers. To reveal the nature of the luminescent center, we measured the EPR spectra of the corresponding samples with the same masses and present the obtained results in the inset of Fig. 4(b). Obviously, the EPR signal intensity tracks with the PL intensity. This provides a good argument that the luminescent center for the ~400 nm PL band is paramagnetic. From the obtained EPR signals, we can calculate the Landé g value in Zeeman interaction term to be 2.0071. In crystalline Al_2O_3, it has experimentally been proven that the F^+ center (single ionized oxygen vacancy) can emit a PL peak at about 413 nm.[15] Du *et al.*[16] have also reported a similar EPR signal with a Landé g value of 2.0085 and considered it to be from the F^+ center in the PAA membrane. Hence, it is reasonable to attribute the PL band to optical transition in the F^+ center located in alumina matrix. The concentration of oxygen vacancy in the alumina is inversely proportional to that of OH^- in the electrolyte.[12] When anodization is conducted under a large current density, the consumption of OH^- increases. As a result, the OH^- concentration is lowered in electrolyte near the anode and large amount of oxygen vacancies are produced in the alumina.[12] This causes a significant increase of the PL intensity, as shown in Fig. 4(b). Here we should point out that in previous work,[16,17] the intensity of the PL band from oxygen vacancies increases in the annealed sample due to the increased oxygen vacancies caused by Al oxidization at alumina/aluminum interface. However, in our present experiments, thick PAA membranes ($>100\ \mu$m) makes the light emission from the alumina/Al interface undetectable. The collected PL signal in the experiments is mainly from oxygen vacancies near the surface layer of a membrane. Such PL obviously has intensity lower in the annealed sample due to annihilation of some oxygen vacancies.[16]

In conclusion, we have fabricated large quantities of individual ANTs using anodization of Al foil in an aged sulfuric acid solution under high anodic voltage. The obtained sample demonstrates a unique three-layer structure, with the ANT array located in the middle layer. We have discussed the formation mechanism of the ANTs. In addition, we have also investigated the blue emission property of all the samples under ultraviolet excitation. Based on annealing behavior of the blue emission band and our EPR result, we have attributed the blue emission to optical transition in the F^+ centers in the alumina matrix.

This work was supported by grants (Nos. 10225416 and BK2006715) from the National and Jiangsu Natural Science Foundations as well as the LAPEM. Partial support was also from the Major State Basic Research Project No. G001CB3095 of China and City University of Hong Kong Direct Allocation Grant No. 9360110.

[1] H. Masuda and K. Fukuda, Science **268**, 1466 (1995).
[2] Z. L. Yang, Z. W. Niu, X. Y. Cao, Z. Z. Yang, Y. F. Lu, Z. B. Hu, and C. C. Han, Angew. Chem. Int. Ed. **42**, 4201 (2003).
[3] G. S. Wu, L. D. Zhang, B. C. Cheng, T. Xie, and X. Y. Yuan, J. Am. Chem. Soc. **126**, 5976 (2004).
[4] K. K. Kim and J. I. Jin, Nano Lett. **1**, 631 (2001).
[5] M. Steinhart, S. Zimmermann, P. Göring, A. K. Schaper, U. Gösele, C. Weder, and J. H. Wendorff, Nano Lett. **5**, 429 (2005).
[6] Y. F. Mei, X. L. Wu, X. F. Shao, G. G. Siu, and X. M. Bao, Europhys. Lett. **62**, 595 (2003).
[7] H. J. de Wit, C. Wijenberg, and C. Crevecoeur, J. Electrochem. Soc. **123**, 1479 (1976).
[8] Y. F. Mei, X. L. Wu, X. F. Shao, G. S. Huang, and G. G. Siu, Phys. Lett. A **309**, 109 (2003).
[9] Z. L. Xiao, C. Y. Han, U. Welp, H. H. Wang, W. K. Kwok, G. A. Willing, J. M. Hiller, R. E. Cook, D. J. Miller, and G. W. Crabtree, Nano Lett. **2**, 1293 (2002).
[10] X. F. Shao, X. L. Wu, G. S. Huang, T. Qiu, M. Jiang, and J. M. Hong, Appl. Phys. A: Mater. Sci. Process. **81**, 621 (2005).
[11] S. Z. Chu, K. Wada, S. Inoue, M. Isogai, and A. Yasumori, Adv. Mater. (Weinheim, Ger.) **17**, 2115 (2005).
[12] G. S. Huang, X. L. Wu, Y. Xie, X. F. Shao, and S. H. Wang, J. Appl. Phys. **94**, 2407 (2003).
[13] G. D. Sulka, S. Stroobants, V. V. Moshchalkov, G. Borghs, and J.-P. Celis, J. Electrochem. Soc. **151**, B260 (2004).
[14] H. Tamura, M. Rückschloss, T. Wirschem, and S. Vepřek, Appl. Phys. Lett. **65**, 1537 (1994).
[15] W. Chen, H. G. Tang, C. S. Shi, J. Dang, J. Y. Shi, Y. X. Zhou, S. D. Xia, Y. X. Wang, and S. T. Yin, Appl. Phys. Lett. **67**, 317 (1995).
[16] Y. Du, W. L. Cai, C. M. Mo, J. Chen, L. D. Zhang, and X. G. Zhu, Appl. Phys. Lett. **74**, 2951 (1999).
[17] Y. Li, G. H. Li, G. W. Meng, L. D. Zhang, and F. Phillipp, J. Phys.: Condens. Matter **13**, 2691 (2001).